

High Nuclearity in Azido/Oximate Chemistry: Ni₁₄ and Ni₁₃ Clusters with *S* = 6 and 9 Ground States

Jordi Esteban,[†] Laura Alcázar,[†] Maria Torres-Molina,[†] Montserrat Monfort,[†] Mercè Font-Bardia,[‡] and Albert Escuer^{*,†}

[†]Departament de Química Inorgànica, Universitat de Barcelona, Av. Diagonal 645, 08028 Barcelona, Spain

[‡]Departament de Mineralogia i Cristal·lografia, Universitat de Barcelona, Martí Franqués s/n, 08028 Barcelona, Spain

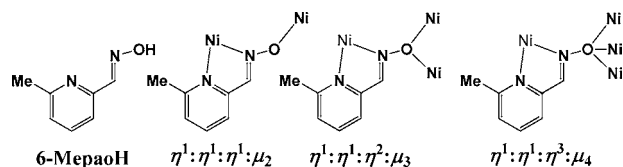
S Supporting Information

ABSTRACT: In the present work, we report a family of Ni₁₄ and unprecedented Ni₁₃ clusters linked by end-on azido and oximate bridges. Ferrimagnetic response gives *S* = 6 and 9 ground states, resulting in the largest nuclearities and spins in nickel oximate chemistry.

Coordination chemistry of salicyl¹ or pyridyl² oximate ligands has grown in the past decade in relation to their ability to generate high-nuclearity metallic clusters with single-molecule-magnet (SMM) response. Blending of different bridging ligands (other than carboxylates) is a synthetic strategy widely employed in cluster chemistry to increase the nuclearity or to improve the magnetic properties of the resulting complexes. The azido anion (in its end-on coordination mode) has been intensely studied to obtain ferro- or ferrimagnetic high-spin systems with a large variety of coligands.³

Following our previous work in nickel/oximate/azido chemistry, we have centered our attention on the poorly explored ligand 6-methylpyridine-2-carbaldehydeoxime (6-MepaoH; Chart 1), for which, in addition to one early

Chart 1. 6-MepaoH Ligand and Coordination Modes Found in 1–3



reported⁴ Ni^{II}₉ cluster, only some Ni₅ and Ni₆ cages⁵ and one (Mn^{II}Mn^{III})_n chain⁶ have been recently characterized by us. The reaction of 6-MepaoH with Ni^{II} salts in the presence of sodium azide yields clusters with the formulas [Ni₁₃(6-Mepao)₁₂(N₃)₈(OH)₆(N-Meen)₂(MeOH)₄] (1·7MeOH·2H₂O; N-Meen = *N*-methylethylenediamine), [Ni₁₃(6-Mepao)₁₂(N₃)₈(OH)₆(MeOH)₈] (2), and [Ni₁₄(6-Mepao)₁₂(N₃)₈(Cl)₂(OH)₄(MeOH)₄(H₂O)₄]Cl₂ (3·7MeOH·2.5H₂O).

Compounds 1–3, together with the previously reported complexes [Ni₁₂Na₂(OH)₄(N₃)₈(pao)₁₂(H₂O)₁₀](OH)₂ (4) and [Ni₁₄(OH)₄(N₃)₈(pao)₁₄(paoH)₂(H₂O)₂](ClO₄)₂ (5),⁷

form a family of ferrimagnetic clusters with common structural features. The maximum ground state *S* = 9 has been found for the Ni₁₃ compounds 1 and 2.

The largest nuclearities reported until now in nickel oximate chemistry were Ni₁₂ and Ni₁₄, which also exhibit the previous record spin *S* = 6.^{7,8} It is worth noting that the nuclearity for Ni₁₃ is extremely rare, and to our knowledge, only one nickel triazole cluster exhibiting this nuclearity has been reported until now.⁹

A first approach to the family of clusters 1–5 can be made by attending to their common structural motifs. All of them contain two hexanuclear Ni₆ rings, which act as complex as the ligand link two Na⁺ cations (Ni₆Na₂, 4), one Ni²⁺ cation (Ni₆NiNi₆, 1 and 2), or two Ni²⁺ cations (Ni₆Ni₂Ni₆, 3 and 5); see Figure 1. In addition to 1–5, one hexanuclear [Mn^{III}Ni₅(N₃)₄(pao)₆(paoH)₂(OH)₂](ClO₄) system with the same local topology and pao[−] ligands has recently been reported.¹⁰

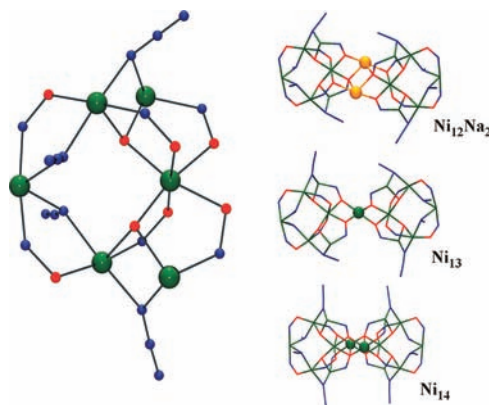


Figure 1. (Left) Plot of the common Ni₆ ring for 1–5. (Right) Schematic core of Ni₁₂Na₂, Ni₁₃, and Ni₁₄ clusters exhibiting a very similar pattern. Color key: Ni, green; O, red; N, blue; Na, orange.

Complexes 1 and 2 are isostructural,¹¹ and thus only 1 will be described in detail. Complex 1 consists of two {Ni₅(6-Mepao)₆(N₃)₄} fragments connected by one nickel linear trinuclear unit (Figure 2). The nickel atoms of these Ni₅ fragments are linked by end-on azido/oximate bridges between

Received: February 22, 2012

Published: May 7, 2012

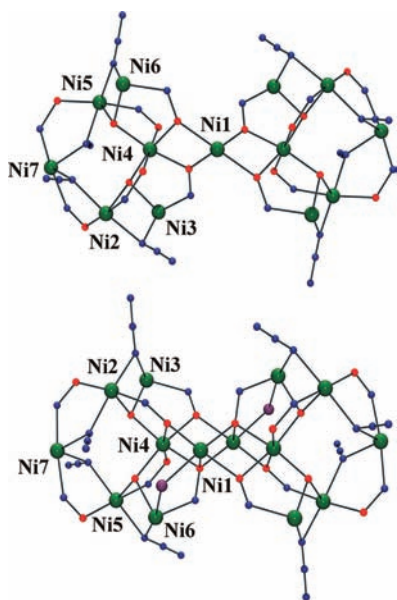


Figure 2. (Top) Core of clusters **1** and **2**. (Bottom) Core of cluster **3**. Color key: Ni, green; O, red; N, blue; Cl, violet.

Ni(2)/Ni(7) and Ni(5)/Ni(7) or end-on azido/hydroxo bridges between Ni(2)/Ni(3) and Ni(5)/Ni(6). Two $\eta^1:\eta^1:\eta^1:\mu_2$ -oximates and two μ_3 -OH bridges link Ni(2,5) with Ni(4), and the core is completed with two $\eta^1:\eta^1:\eta^2:\mu_3$ -oximate bridges [linking Ni(3,6) with Ni(4) and the central Ni(1) atom] and solvent molecules. The N-Meen ligand is linked to Ni(6). The Ni–N–Ni bond angles involving azido ligands show values of $94.6(3)^\circ$ and $99.0(3)^\circ$ for Ni(2)–N–Ni(3) and Ni(5)–N–Ni(6) and larger ones [$111.0(3)^\circ$ and $117.3(3)^\circ$] for Ni(7)–N–Ni(2) and Ni(7)–N–Ni(5). Ni–N–O–Ni torsion angles are lower than 7° except for Ni(3)–N–O–Ni(4), which has a value of $28.5(7)^\circ$. The only difference among **1** and **2** lies in the substitution of the bidentate amine on Ni(6) by two methanol molecules.

Tetradecacomplex **11** **3** is very similar to the previously reported **5**, and the reader can find a detailed description of its core in a corresponding publication.⁷ The main differences are substitution of the neutral bidentate paoH ligands on Ni(2) and the bridging pao[−] bridges in **5** by two methanol molecules and two chloride bridges in **3**. The remaining bond parameters are very similar in both compounds.

The differences between the Ni₁₃ (**1** and **2**) and Ni₁₄ (**3** and **5**) cores are induced by the subtle change in the coordination mode of the 6-Mepao[−] ligands linked to Ni(2) and Ni(6). In the Ni₁₃ cluster, the oxime coordinated to Ni(2) ($\eta^1:\eta^1:\eta^1:\mu_2$ mode) does not interact with the central nickel atom and the oxime coordinated to Ni(6) ($\eta^1:\eta^1:\eta^2:\mu_3$ mode) links Ni(6) with Ni(4) and the central Ni(1) cation. In contrast, in the Ni₁₄ cluster, the oximes coordinated to the Ni(2) and Ni(6) clusters adopts the $\eta^1:\eta^1:\eta^2:\mu_3$ and $\eta^1:\eta^1:\eta^3:\mu_4$ modes, linking Ni(4) and two central atoms Ni(1) and Ni(1') (Figure 3). The increase of the coordination sites in the central fragment of the cluster is fulfilled with the chloro bridges and solvent molecules.

The room temperature $\chi_M T$ value for **1** is $13.7 \text{ cm}^3 \text{ K mol}^{-1}$, close to the expected value for 13 isolated Ni²⁺ ions ($13.0 \text{ cm}^3 \text{ K mol}^{-1}$). Upon cooling, $\chi_M T$ decreases very slightly, exhibiting a broad minimum at 160 K and suggesting ferrimagnetic response. Below the minimum, the plot reaches a maximum $\chi_M T$ value of $20.1 \text{ cm}^3 \text{ K mol}^{-1}$ at 9 K, followed by a fast

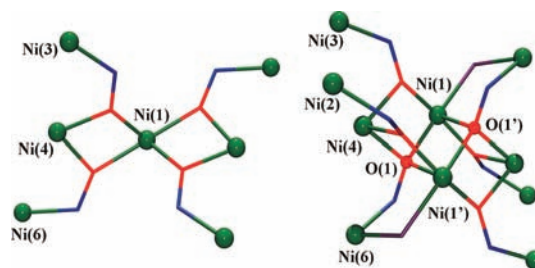


Figure 3. Coordination to the central nickel atoms of the oximate bridging ligands for the Ni₁₃ (left) and Ni₁₄ (right) clusters.

decrease to $12.6 \text{ cm}^3 \text{ K mol}^{-1}$ (Figure 4). Compound **2** shows a quasi-identical behavior (Figure S2 in the Supporting Information).

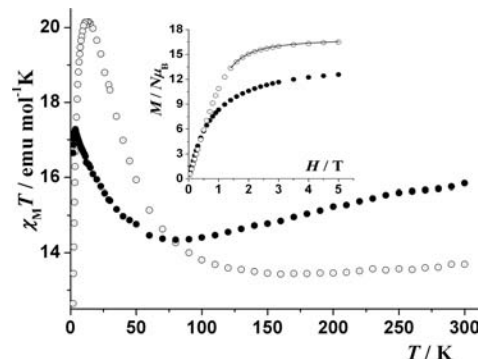


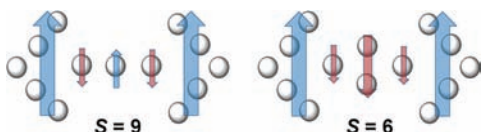
Figure 4. $\chi_M T$ product versus T plot for compounds **1** (open circles) and **3** (solid circles). Inset: magnetization experiments at 2 K showing the high-field fit of the data (solid line).

Compound **3** shows a room temperature $\chi_M T$ value of $15.8 \text{ cm}^3 \text{ K mol}^{-1}$ (slightly larger than that expected for 14 Ni²⁺ isolated ions, $14.0 \text{ cm}^3 \text{ K mol}^{-1}$). $\chi_M T$ decreases upon cooling, exhibiting a clear minimum of $14.3 \text{ cm}^3 \text{ K mol}^{-1}$ at 80 K. Below the minimum, the plot increases up to a maximum $\chi_M T$ value of $17.3 \text{ cm}^3 \text{ K mol}^{-1}$ at 3.7 K and finally slightly diminishes to $16.4 \text{ cm}^3 \text{ K mol}^{-1}$ at 2 K. The size of **1–3** and the large number of superexchange pathways exclude fit of the data, but an approach to the main interactions can be made on the basis of the structural parameters.

As described, these compounds can be envisaged as two pentanuclear Ni^{II} wings linked by a linear Ni₃ or butterfly-like Ni₄ subunits. Nickel atoms from both wings are connected by double oximate/end-on azido or μ_3 -OH/end-on azido bridges. There is experimental evidence that the double oximate/end-on azido bridges promote ferromagnetic coupling,¹² and experimental and theoretical density functional theory calculations also indicate that ferromagnetic coupling should be expected for the double μ_3 -OH/end-on azido bridges.¹³ Thus, we have that each wing should be ferromagnetically coupled with an $S = 5$ local spin. The interaction of Ni(2,3,5,6) with Ni(4), mediated by double $\mu_{2,3}$ -oximate and μ_3 -OH bridges (with Ni–O–Ni angles of around 111° in all cases), should provide an antiferromagnetic contact, and finally the interaction between Ni(4) and Ni(4') with the central Ni(1) atom should be antiferromagnetic in nature according the double Ni–O–Ni linkage with bond angles of $103.2(2)^\circ$ and $109.9(2)^\circ$. Given all of these coupling interactions, we assume that **1** must have a

ground state of $S = 9$ according to the spin alignment shown in Chart 2, left.

Chart 2. Scheme of the Spin Alignment of 1 and 2 (Left) and 3 (Right) and the Proposed Spin Ground States



The lower $\chi_M T$ value observed for **3** is compatible with an $S = 6$ ground state arising from the antiferromagnetic coupling between the ferromagnetic Ni_5 wings and the ferromagnetic central Ni_4 butterfly. This proposal agrees with the $S = 6$ ground state proposed by Christou et al.⁷ for complex **5** and the $S = 3$ ground state reported for the $\{\text{Mn}^{\text{III}}\text{Ni}_5\}$ related system.¹⁰ From experimental evidence, substitution of the oximate bridge in **5** by one bridging chloride in **3** does not modify the magnetic response of the cluster.

This proposal was confirmed by magnetization experiments at 2 K. Magnetization of **1** and **2** shows a fast increase with quasi-saturated values equivalent to 16.5 and 17.2 electrons (Figures 4 and S2 in the Supporting Information). The low-field magnetization of **1** is slightly sigmoidal, showing a maximum at 0.3 T in its first derivative and suggesting an intercluster interaction close to -0.3 cm^{-1} . A fit of the magnetization data above 1.5 T (to discard the intercluster interaction effect) gives an excellent fit for an $S = 9$ spin with a low D value of -0.15 cm^{-1} (Figure 4, inset). Thus, the low- T decay in the $\chi_M T$ plot can be attributed to intercluster interactions mainly mediated by hydrogen bonds. Magnetization for **3** tends to be equivalent to 12.6 electrons, in good agreement with the proposed $S = 6$ ground state and the reported data for **5**.

Despite the large $S = 9$ ground state, the low D value, arising partially from the C_2 symmetry of the molecule, excludes the observation of out-of-phase signals and a SMM response of over 2 K, as was experimentally checked by alternating-current susceptibility measurements.

In conclusion, the new topology of the $\{\text{Ni}_{13}\}$ clusters completes a family of clusters exhibiting the largest nuclearity and spin ground states in nickel/oximate chemistry. These complexes provide new examples of the relevant versatility of the oxime ligands to generate high-nuclearity systems and the ability of the azido ligand to promote selective ferromagnetic interactions.

■ ASSOCIATED CONTENT

Supporting Information

X-ray crystallographic data for complexes **1** and **3** in CIF format, experimental procedures, and structural and magnetic data for compound **2** (Figures S1 and S2). This material is available free of charge via the Internet at <http://pubs.acs.org>.

■ AUTHOR INFORMATION

Corresponding Author

*E-mail: albert.escuer@ub.edu.

Notes

The authors declare no competing financial interest.

■ ACKNOWLEDGMENTS

This work was supported by CICYT Project CTQ2009-07264. A.E. is thankful for financial support from the Excellence in Research ICREA-Academia Award.

■ REFERENCES

- (1) (a) Milios, C. J.; Raptopoulou, C. P.; Terzis, A.; Lloret, F.; Vicente, R.; Perlepes, S. P.; Escuer, A. *Angew. Chem., Int. Ed.* **2004**, *43*, 210. (b) Milios, C. J.; Vinslava, A.; Wood, P. A.; Parsons, S.; Wernsdorfer, W.; Christou, G.; Perlepes, S. P.; Brechin, E. K. *J. Am. Chem. Soc.* **2007**, *129*, 8. (c) Milios, C. J.; Vinslava, A.; Wernsdorfer, W.; Prescimone, A.; Wood, P. A.; Parsons, S.; Perlepes, S. P.; Christou, G.; Brechin, E. K. *J. Am. Chem. Soc.* **2007**, *129*, 6547.
- (2) (a) Milios, C. J.; Stamatatos, Th. C.; Perlepes, S. P. *Polyhedron* **2006**, *25*, 134 (Polyhedron Report). (b) Tasiopoulou, A. J.; Perlepes, S. P. *Dalton Trans.* **2008**, 5537 (Perspective).
- (3) Escuer, A.; Aromi, G. *Eur. J. Inorg. Chem.* **2006**, 4721 (Microreview).
- (4) Pajunen, A.; Mutikainen, I.; Saarinen, H.; Orama, M. Z. *Kristallogr.—New Cryst. Struct.* **1999**, *214*, 217.
- (5) Escuer, A.; Vlahopoulou, G.; Mautner, F. A. *Dalton Trans.* **2011**, *40*, 10109.
- (6) Escuer, A.; Vlahopoulou, G.; Mautner, F. A. *Inorg. Chem.* **2011**, *50*, 2717.
- (7) (a) Stamatatos, T. C.; Abboud, K. A.; Perlepes, S. P.; Christou, G. *Dalton Trans.* **2007**, 3861. (b) Stamatatos, T. C.; Escuer, A.; Abboud, K. A.; Raptopoulou, C. P.; Perlepes, S. P.; Christou, G. *Inorg. Chem.* **2008**, *47*, 11825.
- (8) (a) Papatriantafyllopoulou, C.; Jones, L. F.; Nguyen, T. D.; Matamoros-Salvador, N.; Cunha-Silva, L.; Almeida-Paz, F. A.; Evangelisti, M.; Brechin, E. K.; Perlepes, S. P. *Dalton Trans.* **2008**, 3153. (b) Ji, C.-M.; Yang, H.-J.; Zhao, C.-C.; Tangoulis, V.; Cui, A.-L.; Kou, H.-Z. *Cryst. Growth Des.* **2009**, *9*, 4607. (c) Kou, H.-Z.; An, G.-Y.; Ji, C.-M.; Wang, B.-W.; Cui, A.-L. *Dalton Trans.* **2010**, *39*, 3153.
- (9) (a) Papatriantafyllopoulou, C.; Diamantopoulou, E.; Terzis, A.; Lalioti, N.; Tangoulis, V.; Perlepes, S. P. *Inorg. Chem. Commun.* **2008**, *11*, 454. (b) Papatriantafyllopoulou, C.; Diamantopoulou, E.; Terzis, A.; Tangoulis, V.; Lalioti, N.; Perlepes, S. P. *Polyhedron* **2009**, *28*, 1903.
- (10) Chen, H.; Ma, C.-B.; Yuan, D.-Q.; Hu, M.-Q.; Wen, H.-M.; Liu, Q.-T.; Chen, C.-N. *Inorg. Chem.* **2011**, *50*, 10352.
- (11) Crystal data for $1 \cdot 7 \text{ MeOH} \cdot 2 \text{ H}_2\text{O}$: $\text{C}_{94}\text{N}_{52}\text{Ni}_{13}\text{O}_{22}\text{H}_{116} \cdot (\text{CH}_4\text{O})_7(\text{H}_2\text{O})_2$ (3353.98), monoclinic, $C2/c$, $a = 24.582(13) \text{ \AA}$, $b = 22.488(8) \text{ \AA}$, $c = 27.802(10) \text{ \AA}$, $\beta = 91.96(2)^\circ$, $V = 15360(11) \text{ \AA}^3$, $Z = 4$, $T = 100(2) \text{ K}$, $\lambda(\text{Mo K}\alpha) = 0.71073 \text{ \AA}$, 23067 reflections collected, 14280 unique ($R_{\text{int}} = 0.0446$), $R = 0.0611$, $R_w^2 = 0.1587$. Crystal data for $3 \cdot 7 \text{ MeOH} \cdot 2.5 \text{ H}_2\text{O}$: $\text{C}_{88}\text{H}_{96}\text{Cl}_4\text{N}_{48}\text{Ni}_{14}\text{O}_{24} \cdot (\text{CH}_4\text{O})_7(\text{H}_2\text{O})_{2.5}$ (3497.25), triclinic, $P\bar{1}$, $a = 16.227(1) \text{ \AA}$, $b = 16.709(2) \text{ \AA}$, $c = 19.201(2) \text{ \AA}$, $\alpha = 108.409(5)^\circ$, $\beta = 92.219(5)^\circ$, $\gamma = 115.014(4)^\circ$, $V = 4385.7(7) \text{ \AA}^3$, $Z = 1$, $T = 100(2) \text{ K}$, $\lambda(\text{Mo K}\alpha) = 0.71073 \text{ \AA}$, 17249 reflections collected, 17249 unique ($R_{\text{int}} = 0.0426$), $R = 0.0424$, $R_w^2 = 0.1380$. Cell data for **2**: monoclinic, $C2/c$, $a = 24.525(5) \text{ \AA}$, $b = 22.274(5) \text{ \AA}$, $c = 27.632(6) \text{ \AA}$, $\beta = 92.96(1)^\circ$, $V = 15074(1) \text{ \AA}^3$. CCDC deposition numbers for **1** and **3**: 867793 and 867794.
- (12) (a) Stamatatos, T. C.; Diamantopoulou, E.; Raptopoulou, C. P.; Psycharis, V.; Escuer, A.; Perlepes, S. P. *Inorg. Chem.* **2007**, *46*, 2350. (b) Papatriantafyllopoulou, C.; Stamatatos, T. C.; Wernsdorfer, W.; Teat, S. J.; Tasiopoulos, A.; Escuer, A.; Perlepes, S. P. *Inorg. Chem.* **2010**, *49*, 10486.
- (13) Esteban, J.; Ruiz, E.; Font-Bardia, M.; Calvet, T.; Escuer, A. *Chem.—Eur. J.* **2012**, *18*, 3637.